nzsee
NEW ZEALAND SOCIETY FOR EARTHQUAKE ENGINEERING

Fatigue life assessment of reinforced concrete piers

M. Peat, S. Evans, M. Tripathi & R.P. Dhakal
University of Canterbury, Christchurch.

ABSTRACT

Reinforced concrete (RC) structures subjected to seismic excitation resist lateral-load by undergoing inelastic deformations in their critical regions. This results in the accumulation of low-cycle fatigue damage in reinforcing bars and increases the likelihood of premature failure in future earthquakes and aftershocks. Therefore, this paper investigates the combined effect of bar buckling and low-cycle fatigue damage on the remaining life of RC bridge piers. For this purpose, a numerical model capable of simulating the seismic response of RC bridge piers is developed and non-linear time history analysis is carried out. A suite of ground motions representing the seismicity in Wellington CBD is adopted for numerical analysis. Reinforcing bar strain histories are extracted from the numerical analysis, and accumulated damage in the plastic hinge regions of the column is evaluated. Further, a novel fatigue life model that incorporates the effect of bar buckling on fatigue life of reinforcing bars is implemented and effect of bar buckling on the remaining life of a typical RC bridge pier is analytically evaluated. Comparative evaluation of the numerical results is carried out and effect of ground motion intensity and transverse reinforcement detailing (represented by the bar buckling length) on the remaining life of RC bridge piers is quantified.

1 INTRODUCTION

During moderate to large seismic events, reinforced concrete (RC) structures undergo inelastic deformations accompanied by damage. Non-linear response of RC structures depends on the inelastic deformations in their critical regions; i.e. *plastic hinge regions*. In these critical regions, reinforcing bars are subject to large inelastic tensile and compressive strain reversals resulting in the accumulation of low-cycle fatigue damage, which results in their premature fracture.

Low-cycle fatigue damage of reinforcing bars is one of the commonly observed failure modes in flexural RC members [1-3]. Accumulation of inelastic tensile strains in reinforcing bars can continue during aftershocks following the main event, thereby further deteriorating the seismic performance of RC structures and increasing the probability of premature failure or collapse in future events. Performance of RC structures in past earthquakes have highlighted the importance of premature bar fracture, wherein bar fracture has been primarily caused either due to a concentration of large tensile strains (across a single large crack in RC

members with low-reinforcement ratio) or due to fatigue failure accelerated by bar buckling as a result of poor detailing of transverse reinforcement [4].

In the past, several investigations have resulted in the development of low-cycle fatigue life models for reinforcing bars. Mander et al. [5] developed a fatigue model for ASTM A722 type II and A615 Grade 40 based on the total and plastic strain amplitude, and dissipated energy. Another fatigue life model was developed by Brown and Kunnath [6] by testing ASTM A615 reinforcing bars of varying diameters. Similarly, Hawileh et al. [7] tested ASTM A706 and A615 Grade 60 reinforcing bars under fatigue loading and developed fatigue life material models. Although it has been well acknowledged that bar buckling has a detrimental effect on fatigue life of the reinforcing bars, none of the above-discussed fatigue models accounts for this detrimental effect. Therefore, recent studies have focused on evaluating the effect of bar buckling on the fatigue life of reinforcing bars [8-10]. Kashani et al. [8] investigated the fatigue response of British smooth and ribbed reinforcing bars and developed an analytical model that incorporates the effect of bar buckling on fatigue life of reinforcing bars. More recently, Tripathi et al. [9] investigated the effect of bar buckling on low-cycle fatigue life of New Zealand reinforcing bars. For this purpose, New Zealand Grade 300E and 500E reinforcing bars were tested under fatigue loading and a low-cycle fatigue model that relates the fatigue life of reinforcing bars and total strain amplitude as a function of bar buckling was proposed.

The remaining life assessment of RC structures have been of interest to many researchers in the past; however, in most of these reported studies, the detrimental effect of bar buckling on the fatigue life of reinforcing bars was not considered. Therefore, this paper investigates the effect of bar buckling and low-cycle fatigue damage on the remaining life of RC bridge piers. For this purpose, non-linear fibre-element modelling of a typical bridge pier is developed to carry out non-linear time-history analyses. A generic process is formulated to estimate low-cycle fatigue damage of reinforcing bars in RC structures using the number and magnitude of strain cycles experienced by the bars within a response history, which is used to estimate the remaining life of a typical bridge pier following different ground motions.

2 NUMERICAL INVESTIGATIONS

To investigate the combined effect of bar buckling and low-cycle fatigue on the remaining life of RC members, a typical RC bridge pier was modelled using fibre-element technique and analysed using the finite element analysis program OpenSees [11]. In non-linear fibre-element modelling of structural members, RC members are represented as a series of single-line elements, and each element's cross-section is discretised into core concrete, unconfined concrete and reinforcement fibres (as shown in Figure 2). In this modelling approach, the global response of an RC member is obtained by integrating the uniaxial behaviour of concrete and reinforcing fibres. Therefore, the reliability of a fibre-element model to simulate non-linear response is dependent on the ability of the adopted material models to realistically simulate the cyclic response of RC materials. In this study, the response of confined concrete was modelled using the stress-strain model proposed by Mander et al. [12] and implemented in OpenSees as the material model Concrete02 [11], as shown in Figure 1a. The stress-strain response of reinforcing bars was modelled using the model developed by Menegotto and Pinto [13] and implemented in OpenSees as Steel02 uniaxial material [11], as shown in Figure 1b. It should be noted that the reinforcing bar material model adopted in this study does not incorporate the cumulative effect of buckling on the stress-strain relationship of the reinforcement, and is acknowledged as one of the key limitations of this modelling strategy. Nevertheless, in this study, the combined effect of buckling and low-cycle fatigue on the remaining life of the RC column is incorporated by post-processing the analysis results, and the detailed procedure for the same is discussed in subsequent sections.

2.1 Model Validation

In order to validate the efficacy of the adopted modelling approach, one of the previously tested RC columns from the published literature was adopted and nonlinear analysis was carried out. For this purpose, Column A2 tested by Kunnath et al. [14] was adopted. Column A2 was a one-fourth scale model of a prototype bridge pier and was 1372 mm high and 305 mm in diameter. Figure 3 shows the cross-sectional detailing of Column A2. A constant axial load of 200 kN was applied before the application of incremental unidirectional lateral cyclic loading. The failure of column A2 was governed by flexural failure modes including concrete spalling, concrete crushing, and bar buckling and fracture. Figure 3 shows the comparison of analytical and numerical test results. As can be seen from this figure, the numerical model was reasonably able to predict the hysteretic response of column A2. Therefore, this modelling strategy (as described above) has been adopted for conducting fatigue life assessment of RC bridge pier in this study.

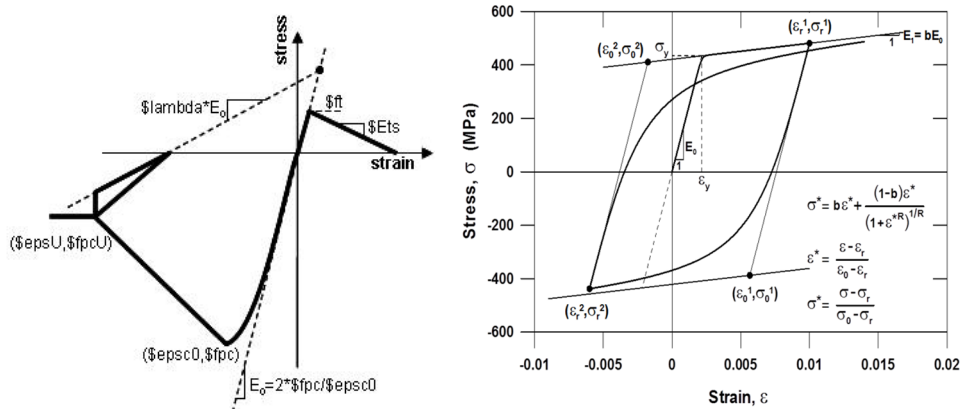

(a) Concrete material model *(b) Steel material model*

Figure 1: Uniaxial constitutive material models used in numerical analysis OpenSees [11]

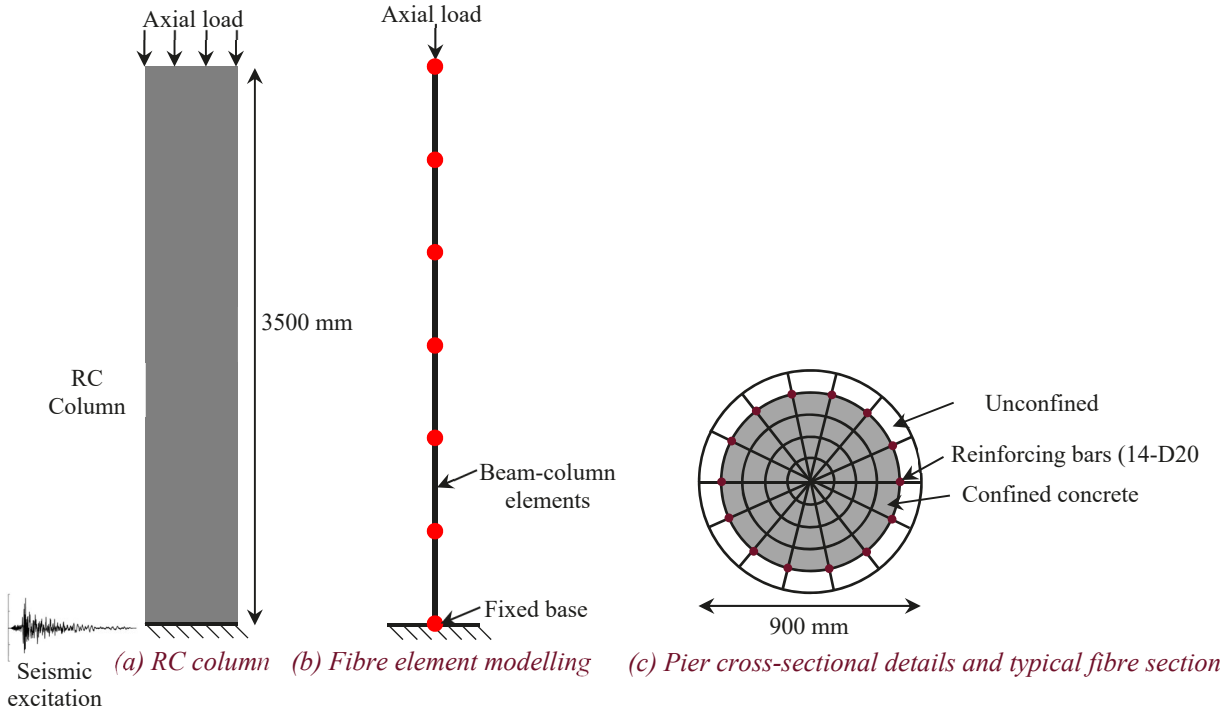

(a) RC column *(b) Fibre element modelling* *(c) Pier cross-sectional details and typical fibre section*

Figure 2: Schematic layout of the fibre element modelling and details of the analysed RC column

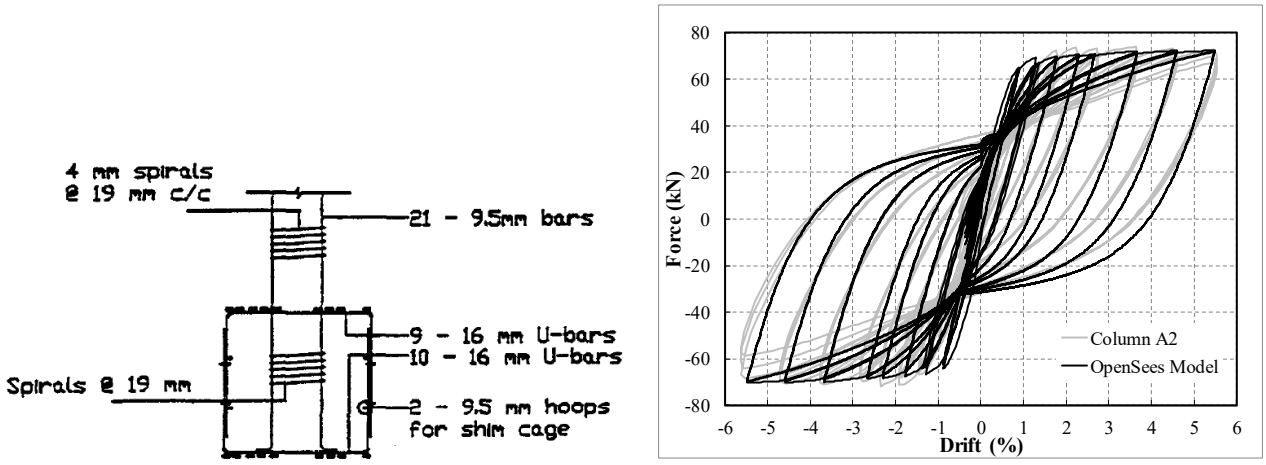

(a) Column A2 *(b) Hysteretic response of Column A2*

Figure 3: Comparative evaluation of experimental and analytical global hysteretic response

2.2 Details of the Adopted RC Bridge Pier and Fatigue Assessment Strategy

The bridge pier selected for the numerical analysis represented a typical bridge pier located in the Wellington region and designed according to New Zealand Standards. With an estimated deck weight of 780 kN, the selected circular bridge pier was 900 mm wide and 3500 mm high and was reinforced with fourteen D20 longitudinal reinforcing bars. Figure 2 shows the geometry and reinforcing arrangement of the identified pier.

A parametric study was conducted to investigate the effect of bar buckling and earthquake intensity on residual life of the RC bridge pier. For this purpose, the bridge pier was subjected to several ground motions with increasing intensities and the strain histories from the extreme reinforcing bars were recorded and processed to estimate the fatigue damage accumulated in these bars. Thereafter, the commonly used Rainflow cycle counting algorithm was used [15] to count the equivalent number of cycles and corresponding amplitudes.

As highlighted earlier, most of the fatigue life models do not incorporate the effect of bar buckling on accelerated fatigue damage accumulation in reinforcing bars. Therefore, in this study, the fatigue life model developed by Tripathi et al. [9] was used to account for the effect of bar buckling on fatigue life of reinforcing bars. Tripathi et al. [9] developed an analytical fatigue life model that incorporated the effect of inelastic buckling based on tests carried out on New Zealand reinforcing bars with different slenderness ratios. According to this model, the fatigue life of reinforcing bars can be estimated using Equation 1.

$$\varepsilon_a = \beta\left(2N_f\right)^a \tag{1}$$

Where ε_a is the total strain amplitude, $2N_f$ is the number of half-cycles to failure, β is the fatigue ductility coefficient given by Equation 2, and a is the fatigue ductility exponent given by Equation 3.

$$\beta = \frac{-\lambda}{350} + 0.2 \tag{2}$$

$$a = \left(\frac{\lambda}{1200} + 0.441\right) \tag{3}$$

In the above equations, λ is a non-dimensional buckling parameter that defines the buckling tendency of a reinforcing bar and can be estimated using Equation 4. It should be noted that in Equation 4, L is not the spacing between the transverse reinforcement but is the total buckling length of reinforcing bars which can extend to multiple tie spacings in mm, D is the diameter of the longitudinal reinforcement in mm and f_y is the yield strength in MPa (300 MPa) [16]. Herein, the buckling length of a reinforcing bar (L) can be estimated by using the bar stability model proposed by Dhakal and Maekawa [16].

$$\lambda = \frac{L}{D}\sqrt{\frac{f_y}{100}} \tag{4}$$

After estimating the number of half-cycles and corresponding strain amplitudes, the fatigue damage is determined using Miner's linear damage hypothesis [17]. The incremental fatigue damage (ΔD_i) caused due to one half-cycle of 'ε_{a1}' strain amplitude is estimated using Equation 5, and the total cumulative damage is estimated using Equation 6. Herein, cumulative damage of zero and one represent a virgin bar (only in terms of fatigue damage) and a fatigue-fractured bar, respectively.

$$\Delta D_i = \frac{1}{\left(\frac{\varepsilon_{a1}}{\beta}\right)^{\frac{1}{a}}} \tag{5}$$

$$D = \Delta D_i + \Delta D_{i-1} \tag{6}$$

2.3 Ground Motion Selection and Scaling

A set of 20 ground motion time histories were selected to represent the median target response spectral shape in Wellington. The ground motions were processed using SeismoSoft [18] to produce the target acceleration response spectrum for the Wellington region. The Wellington region target spectra was calculated considering Soil Class C and a Hazard Factor (Z) of 0.4 using Equation 7 [19].

$$S_{ATarget} = \left(\frac{1+S_p}{2}\right) C(T) Z \tag{7}$$

The selected ground motions were scaled using the ground motion scaling approach specified in NZS1170.5 [19], the scale factor (k_1) was determined for each ground motion to scale the record to match with the 500-year return period target spectra within a period range of 0.16 s – 0.52 s (i.e. 0.4-1.3 times the natural period of 0.4 s). Figure 4a shows a plot of all ground motions scaled to represent the target spectra for a 500-year return period. Three intensity levels are considered in the analysis corresponding to a return period of 500, 1000 and 2500 years. These three levels of intensity were produced by scaling each ground motion by the return period factor (R). Four ground motions, whose spectral shapes conflicted the target spectra due to extreme peaks and troughs, were discarded during the scaling process. Figure 4b shows the scaling factors for the sixteen selected ground motions corresponding to three different intensity levels.

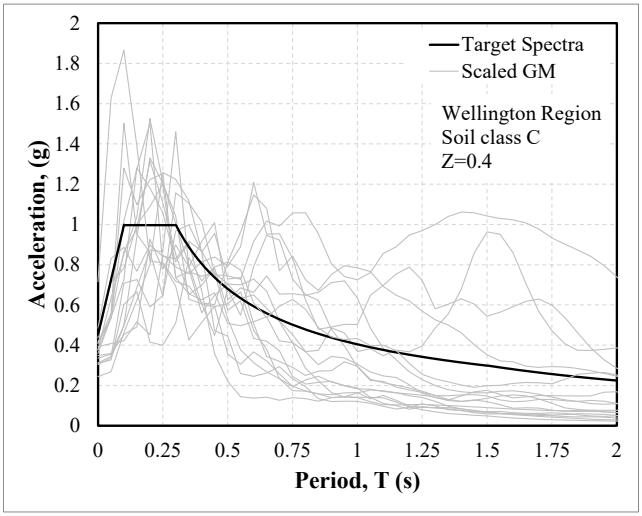

(a) Target spectra 500-year return period

GM	$k_{1,1/500}$	$k_{1,1/1000}$	$k_{1,1/2500}$
1	2.49	3.23	4.48
2	1.31	1.70	2.35
3	2.44	3.17	4.39
4	2.22	2.89	4.00
5	1.12	1.46	2.02
6	1.91	2.48	3.44
7	1.70	2.21	3.06
8	1.73	2.25	3.11
9	0.83	1.08	1.49
10	2.95	3.83	5.30
11	0.67	0.87	1.21
12	2.29	2.98	4.12
13	0.75	0.98	1.35
14	2.04	2.65	3.67
15	0.58	0.76	1.05
16	0.79	1.03	1.42

(b) Ground motion scaling factors

Figure 4: Ground motion scaling

3 RESULTS AND DISCUSSION

3.1 Hysteretic Response

Non-linear time history analysis using the bridge pier's fibre-element model was conducted for all ground motions scaled to different intensity levels. Figure 5 and Figure 6 compare the hysteretic response of the bridge pier subjected to a typical ground motion GM08 with three different ground motion intensities corresponding to 1/500, 1/1000 and 1/2500 annual exceedance probability (AEP). As can be seen from this figure, increasing the earthquake intensity substantially increases the lateral deformation of the bridge pier and subsequently increases the concentration of nonlinear strain in the plastic hinge region.

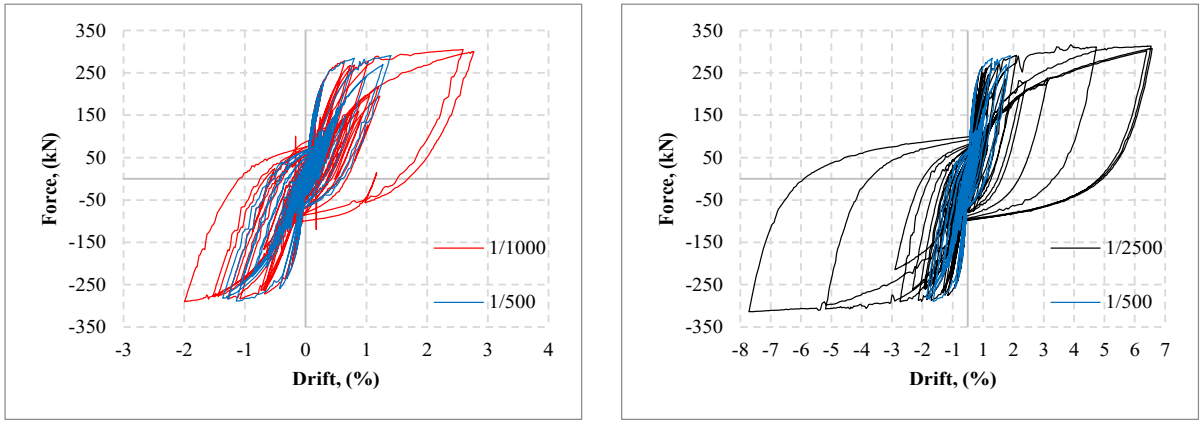

(a) *(b)*

Figure 5: GM08 Force-displacement of the bridge pier for 500, 1000 and 2500-year return period earthquakes

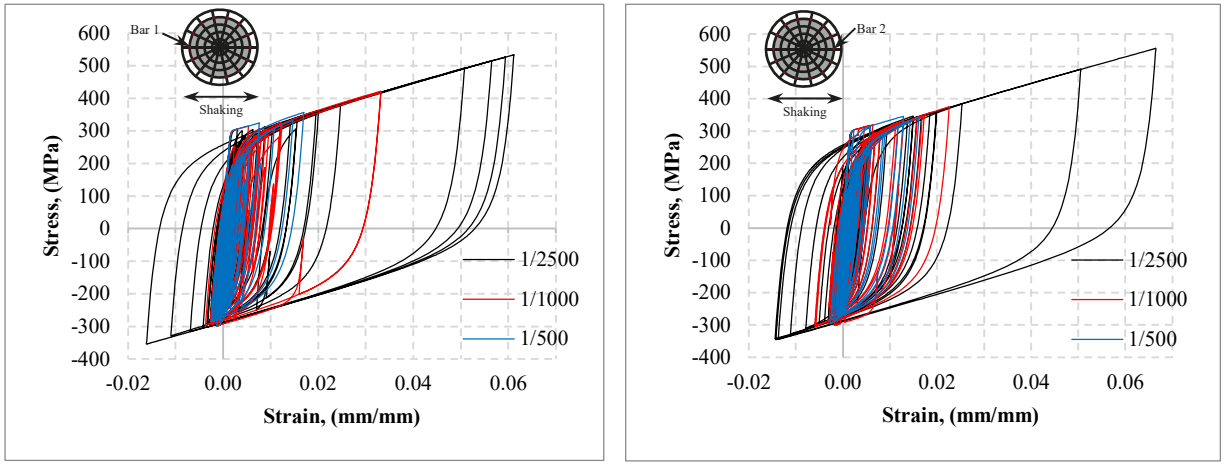

(a) Reinforcing bar 1 *(b) Reinforcing bar 2*

Figure 6: GM08 Stress-strain history for extreme reinforcing bars

3.2 Effect of Ground Motion Intensity on Strain History

Figure 7 shows the strain histories for reinforcing bars 1 and 2 produced by GM08 at each of the three intensity levels. Note that the yield strain of normal strength steel bars is about 0.0015, which is well exceeded in all three response strain histories. There is a clear difference in the strain histories for bars 1 and 2, as shown in Figure 7a and 7b. Even though the two extreme bars are subject to the same ground motion, the acceleration history is not symmetrical in the direction of shaking. Therefore, the two bars are subjected to different amounts of extension and compression during the acceleration reversals resulting in different accumulated damage.

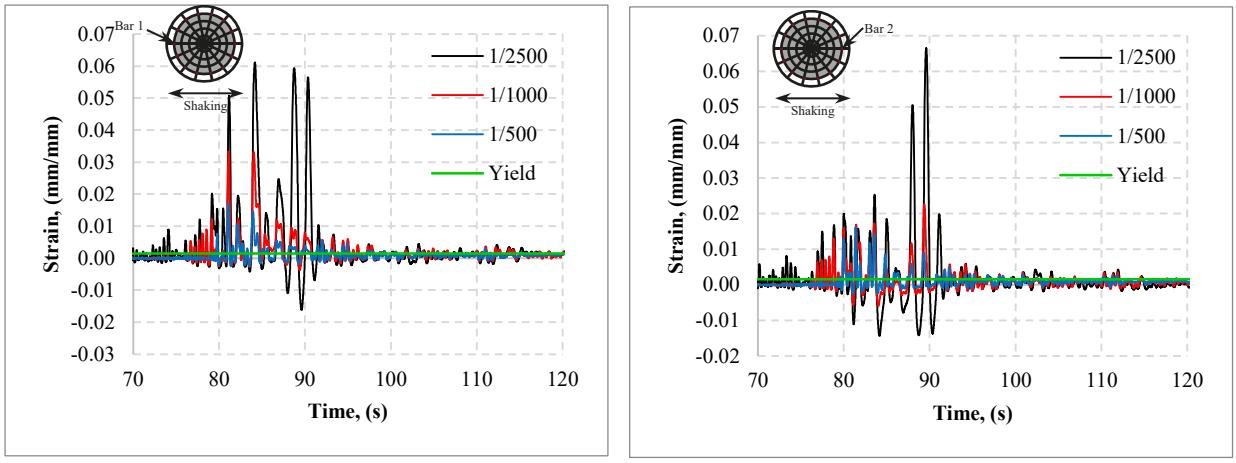

(a) Reinforcing bar 1 *(b) Reinforcing bar 2*

Figure 7: Strain history of the extreme bars in the pier subjected to GM08

3.3 Damage Results

The strain histories recorded from the numerical analyses were post-processed to identify the strain reversal points to ascertain the strain amplitude and the corresponding number of cycles. Following this, the cumulative damage was calculated for all combinations of the sixteen-ground motion, three different intensities, and five different slenderness (L/D) ratios (6, 9, 12, 15 and 24). The damage calculation was carried out for both bar 1 and bar 2, and the final damage results are summarised in Table 1. The large difference between the damages for each intensity, as shown in Table 1, can be explained by looking at the strain history for GM08 in Figure 7. The number, and most importantly, the amplitude of inelastic strain cycles is much higher for a 2500-year return period ground motions as compared to the 500 and 1000-year motions. In addition to this, the bracketed duration of the strain history increases with increased intensity. Herein, the bracketed duration is defined as the duration between the first and last instances when the strain amplitude exceeds the yielding strain. As can be seen in Table 1, the difference between the response and damage sustained by the two extreme bars, as identified in Figure 7 for GM08, is also apparent for all combinations of ground motions, intensity levels and slenderness ratios.

3.4 Effect of Ground Motion Intensity on Fatigue Damage

The intensity of ground motion has a direct impact on the extent of fatigue damage (and hence the residual fatigue life) of an RC structure. The effect of ground motion intensity on the bridge pier was investigated herein for all 16 ground motions. Probabilistic curves were generated to compare the three ground motion intensity levels (500, 1000 and 2500-year return period earthquakes). The damage results for each intensity were taken from Table 1, sorted by increasing damage, and the cumulative probability of fatigue damage were derived as shown in Figure 8 for the three intensity levels for L/D ratios of 12 and 24, respectively.

Figure 8 highlights how an increase in earthquake intensity also increases cumulative fatigue damage in the bridge pier. The median damage for an L/D ratio of 24 was 0.076, 0.130, and 0.25 for 500, 1000, and 2500-year return period earthquakes, respectively. An increase from 1/500 to 1/1000 AEP corresponds to a 71% increase in median fatigue damage whilst an increase from 1/1000 to 1/2500 AEP corresponds to a 92% increase in median damage for L/D of 24.

Table 1: Summary of damages for all GMs, intensities and L/D ratios for bar 1 and bar 2

AEP = 1/500	L/D = 6		L/D = 9		L/D = 12		L/D = 15		L/D = 24	
GM	**Bar 1**	**Bar 2**	**Bar 1**	**Bar 2**	**Bar 1**	**Bar 2**	**Bar 1**	**Bar 2**	**Bar 1**	**Bar 2**
1	0.0079	0.0090	0.010	0.012	0.014	0.016	0.019	0.022	0.059	0.065
2	0.00012	0.00010	0.00016	0.00014	0.00022	0.00020	0.00032	0.00028	0.0011	0.00097
3	0.048	0.041	0.062	0.053	0.082	0.071	0.11	0.095	0.33	0.28
4	0.014	0.0066	0.018	0.0087	0.025	0.012	0.033	0.016	0.098	0.050
5	0.0061	0.0071	0.0081	0.009	0.012	0.013	0.015	0.017	0.046	0.053
6	0.0080	0.011	0.011	0.014	0.014	0.019	0.020	0.026	0.061	0.079
7	0.022	0.020	0.029	0.027	0.039	0.036	0.054	0.049	0.16	0.15
8	0.011	0.013	0.015	0.017	0.020	0.023	0.027	0.031	0.081	0.094
9	0.0094	0.012	0.013	0.016	0.017	0.021	0.023	0.029	0.073	0.091
10	0.011	0.0085	0.014	0.011	0.019	0.016	0.027	0.022	0.085	0.070
11	0.0081	0.0070	0.011	0.0094	0.015	0.013	0.020	0.018	0.064	0.056
12	0.054	0.035	0.070	0.045	0.091	0.060	0.12	0.080	0.35	0.23
13	0.012	0.017	0.016	0.023	0.022	0.030	0.030	0.041	0.091	0.12
14	0.0087	0.00870	0.01160	0.01160	0.01560	0.01570	0.02160	0.02160	0.06770	0.06790
15	0.0036	0.0025	0.0048	0.0033	0.0065	0.0045	0.0089	0.0062	0.028	0.020
16	0.017	0.015	0.023	0.020	0.030	0.027	0.042	0.037	0.13	0.11
AEP = 1/1000	**L/D = 6**		**L/D = 9**		**L/D = 12**		**L/D = 15**		**L/D = 24**	
GM	**Bar 1**	**Bar 2**	**Bar 1**	**Bar 2**	**Bar 1**	**Bar 2**	**Bar 1**	**Bar 2**	**Bar 1**	**Bar 2**
1	0.012	0.015	0.016	0.019	0.021	0.025	0.028	0.034	0.085	0.10
2	0.00012	0.00010	0.00017	0.00014	0.00023	0.00020	0.00034	0.00029	0.0012	0.0010
3	0.12	0.10	0.16	0.13	0.21	0.17	0.28	0.23	0.79	0.66
4	0.055	0.022	0.070	0.029	0.091	0.038	0.12	0.051	0.34	0.15
5	0.0073	0.010	0.0096	0.014	0.013	0.018	0.018	0.025	0.055	0.075
6	0.013	0.015	0.017	0.020	0.023	0.026	0.032	0.036	0.096	0.11
7	0.052	0.065	0.068	0.084	0.090	0.11	0.12	0.15	0.36	0.43
8	0.041	0.030	0.053	0.039	0.069	0.052	0.093	0.070	0.27	0.21
9	0.018	0.021	0.023	0.028	0.031	0.038	0.043	0.051	0.13	0.16
10	0.014	0.016	0.019	0.022	0.025	0.030	0.035	0.041	0.11	0.13
11	0.013	0.0098	0.018	0.013	0.024	0.018	0.032	0.024	0.10	0.076
12	0.11	0.064	0.13	0.083	0.17	0.11	0.23	0.15	0.65	0.42
13	0.021	0.025	0.027	0.032	0.036	0.043	0.049	0.058	0.15	0.17
14	0.010	0.010	0.013	0.014	0.018	0.019	0.025	0.026	0.076	0.079
15	0.0032	0.0029	0.0043	0.0039	0.0058	0.0052	0.0080	0.0072	0.025	0.023
16	0.045	0.055	0.059	0.071	0.078	0.094	0.10	0.13	0.31	0.37
AEP = 1/2500	**L/D = 6**		**L/D = 9**		**L/D = 12**		**L/D = 15**		**L/D = 24**	
GM	**Bar 1**	**Bar 2**	**Bar 1**	**Bar 2**	**Bar 1**	**Bar 2**	**Bar 1**	**Bar 2**	**Bar 1**	**Bar 2**
1	0.027	0.037	0.035	0.048	0.046	0.063	0.063	0.084	0.18	0.24
2	0.0014	0.0015	0.0019	0.0020	0.0028	0.0028	0.0037	0.0039	0.012	0.013
3	0.28	0.24	0.35	0.30	0.45	0.39	0.60	0.52	1.0	1.0
4	0.094	0.064	0.12	0.082	0.16	0.11	0.21	0.14	0.57	0.40
5	0.013	0.015	0.017	0.020	0.023	0.026	0.031	0.036	0.094	0.11
6	0.026	0.023	0.034	0.030	0.044	0.040	0.062	0.055	0.18	0.16
7	0.10	0.13	0.13	0.16	0.17	0.21	0.23	0.28	0.67	0.80
8	0.25	0.19	0.31	0.24	0.40	0.31	0.53	0.41	1.0	1.0
9	0.041	0.053	0.054	0.068	0.072	0.091	0.098	0.12	0.30	0.36
10	0.027	0.033	0.036	0.044	0.049	0.059	0.067	0.081	0.21	0.25
11	0.021	0.019	0.027	0.025	0.036	0.033	0.050	0.046	0.15	0.14
12	0.30	0.20	0.38	0.26	0.49	0.33	0.64	0.44	1.0	1.0
13	0.053	0.034	0.068	0.045	0.089	0.059	0.12	0.080	0.35	0.23
14	0.014	0.015	0.018	0.020	0.024	0.027	0.033	0.036	0.10	0.11
15	0.0064	0.0037	0.0084	0.0049	0.0113	0.0066	0.015	0.0091	0.047	0.028
16	0.099	0.12	0.13	0.16	0.17	0.21	0.22	0.27	0.64	0.78

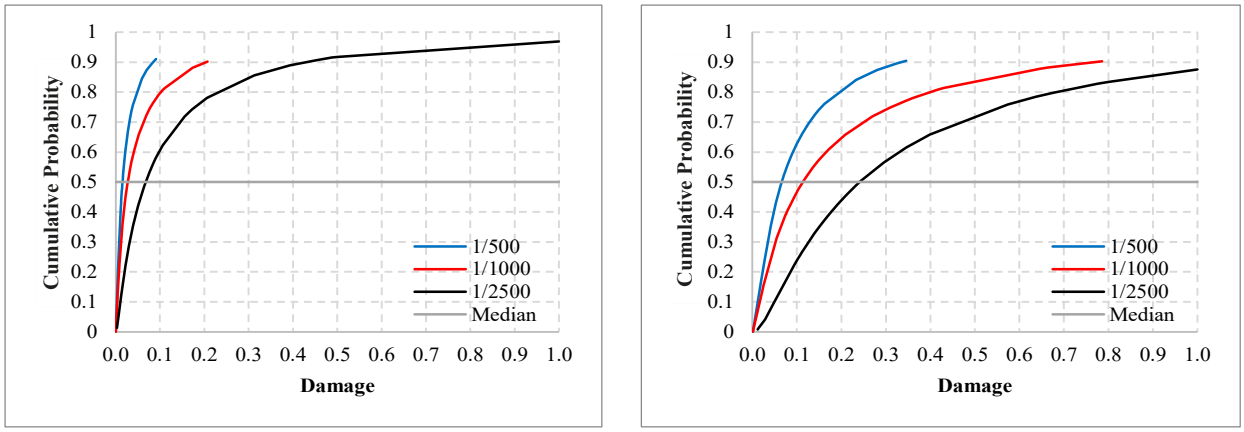

(a) Slenderness ratio, L/D=12 *(b) Slenderness ratio, L/D=24*

Figure 8: Cumulative probability of damage for 500, 1000 and 2500-year return period earthquakes

3.5 Effect of Anti-Buckling Reinforcement Detailing on Fatigue Damage

The performance of RC structures under intense seismic shaking is dictated by how well the critical plastic regions of the structure are detailed. In the fatigue damage calculation procedure, the level of detailing is represented by the non-dimensional buckling parameter, λ (Equation 4), which depends on the buckling length to bar diameter ratio, L/D. The detailing of transverse anti-buckling reinforcement governs the buckling length and hence directly affects how well the pier can perform in the inelastic range of response. To investigate the effect that detailing has on the residual fatigue life of the structure, the analysis was repeated for L/D ratios of 6, 9, 12, 15, and 24. Figure 9 shows the effect of detailing on cumulative damage for 1000 and 2500-year return period earthquakes.

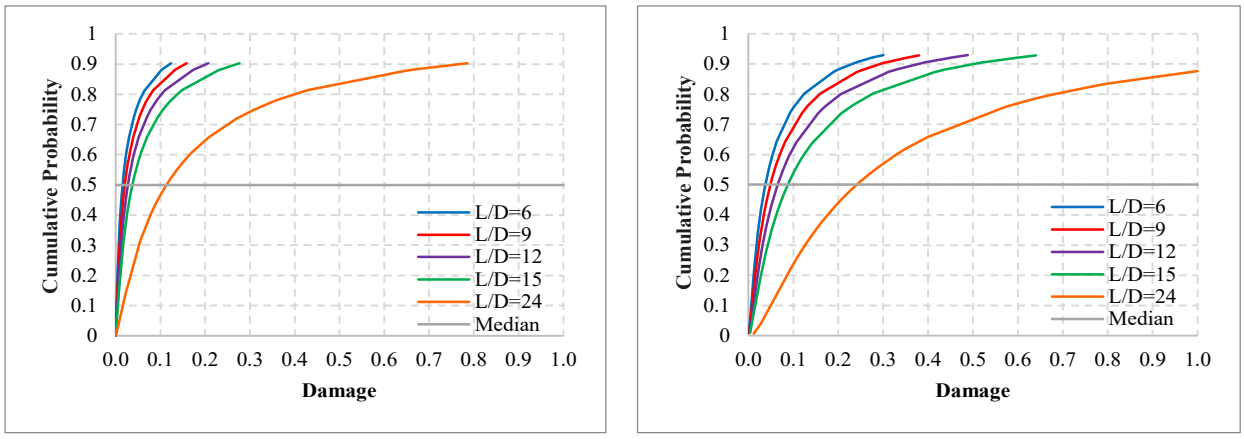

(a) 1000-year return period earthquakes *(b) 2500-year return period earthquakes*

Figure 9: Cumulative probability of damage for varying L/D

The adverse effect of poor detailing on fatigue damage is obvious in Figure 9. The relationship between cumulative damage and slenderness ratio (L/D) of reinforcing bars is not proportional. For an AEP of 1/2500, the median fatigue damage of the pier was 0.061 and 0.25 for the L/D ratio of 12 and 24, respectively. The increase in damage is clearly non-linear as doubling the buckling length resulted in a four-fold increase in the fatigue damage. Additionally, Figure 9 reiterates that as ground motion intensity increases, the probability of exceeding a certain damage state also increases. For example, in Figure 9a with an AEP of 1/1000, there is an 80% chance that the fatigue damage of the pier with an L/D ratio of 24 is less than 0.4. In other words, it indicates 80% confidence that the residual fatigue life (i.e., one minus the cumulative fatigue damage) of the pier is greater than or equal to 60%. However, Figure 9b indicates that with an AEP of 1/2500, the same

confidence drops to 66%. Figure 10 shows a 3-D surface plot of how the median cumulative damage varies with changing slenderness ratio and earthquake intensity.

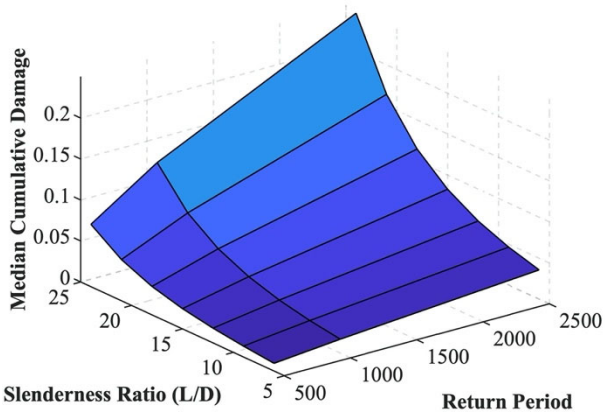

Figure 10: Surface plot of median cumulative damage, slenderness ratio, and earthquake intensity

4 CONCLUDING REMARKS

In this study, the effect of bar buckling and low-cycle fatigue on residual life of an RC bridge pier was numerically investigated. A fibre-element model capable of reliably simulating the response of flexural RC members was developed and non-linear time history analysis was carried out. The key parameters considered for the analytical simulation included ground motions (sixteen ground motions), ground motion intensity (500, 1000 and 2500-year return period earthquakes) and slenderness ratio of reinforcing bars (6, 9, 12, 15 and 24). Based on the results of this study, the following conclusions can be made:

1. The methodology used in this study to estimate fatigue damage of an RC bridge pier seems to be readily applicable to all kinds of RC structures (including multi-story buildings); however, its reliability for other types of structures need to be verified. The applicability of this methodology to different RC Structures will enable estimation of residual fatigue life after a series of earthquakes (or an earthquake sequence).
2. As expected, the study confirmed that increasing ground motion intensity increases the probability of exceeding a certain fatigue-damage limit state in an RC structure. For example, for the analysed bridge pier with L/D of 24, there is 80% confidence that the residual fatigue life will be at least 60% after a 1000-year return period ground motion compared to only 34% for an AEP of 1/2500.
3. The effect of detailing was investigated by repeating the analysis for L/D ratios of 6, 9, 12, 15, and 24. The relationship between the fatigue-damage and L/D ratio is found to become highly non-linear for larger values of L/D. For instance, the median fatigue-damage of the pier with an L/D ratio of 12 and 24 was 0.061 and 0.25, respectively. This indicates that improving the arrangement and detailing of transverse anti-buckling reinforcement can hugely improve the fatigue life of RC piers in high-seismic regions.

The investigations presented in the present paper are a part of a multi-objective research project that aims at quantifying the combined effect of bar buckling and low-cycle fatigue on the seismic performance of RC structures. For this purpose, work is currently underway to implement a novel material model in OpenSees that incorporates the combined effect of bar buckling and low-cycle fatigue and further results will be presented in future publications.

5 REFERENCES

[1] M. Tripathi, R.P. Dhakal, F. Dashti, Bar buckling in ductile RC walls with different boundary zone detailing: Experimental investigation, Engineering Structures 198 (2019).
[2] M. Tripathi, R.P. Dhakal, F. Dashti, Nonlinear cyclic behaviour of high-strength ductile RC walls: Experimental and numerical investigations, Engineering Structures 222 (2020).
[3] M. Tripathi, Bar buckling in ductile reinforced concrete walls: Causes, consequences and control, Department of Civil and Natural Resources Engineering, University of Canterbury, 2020.
[4] M. Tripathi, R.P. Dhakal, Designing and detailing transverse reinforcement to control buckling-induced failure in rectangular RC walls, Bulletin of New Zealand Society for Earthquake Engineering (Accepted) (2021).
[5] J.B. Mander, F.D. Panthaki, A. Kasalanati, Low-cycle fatigue behavior of reinforcing steel, Journal of Materials in Civil Engineering 6(4) (1994) 453-468.
[6] J. Brown, S.K. Kunnath, Low-cycle fatigue failure of reinforcing steel bars, ACI Materials Journal 101(6) (2004) 457-466.
[7] R. Hawileh, A. Rahman, H. Tabatabai, Evaluation of the low-cycle fatigue life in ASTM A706 and A615 Grade 60 steel reinforcing bars, Journal of Materials in Civil Engineering 22(1) (2010) 65-76.
[8] M.M. Kashani, A.K. Barmi, V.S. Malinova, Influence of inelastic buckling on low-cycle fatigue degradation of reinforcing bars, Construction and Building Materials 94 (2015) 644-655.
[9] M. Tripathi, R.P. Dhakal, F. Dashti, L.M. Massone, Low-cycle fatigue behaviour of reinforcing bars including the effect of inelastic buckling, Construction and Building Materials 190 (2018) 1226-1235.
[10] M. Tripathi, R.P. Dhakal, F. Dashti, L.M. Massone, Experimental investigation on low-cycle fatigue life of reinforcing bars, 7th Asia Conference on Earthquake Engineering, Bangkok, Thailand, 2018.
[11] S. Mazzoni, F. McKenna, M.H. Scott, G.L. Fenves, OpenSees command language manual, (2006).
[12] J.B. Mander, M.J. Priestley, R. Park, Theoretical stress-strain model for confined concrete, Journal of structural engineering 114(8) (1988) 1804-1826.
[13] M. Menegotto, P. Pinto, Method of analysis for cyclically loaded RC plane frames including changes in geometry and non-elastic behavior of elements under combined normal force and bending, Proc. of IABSE symposium on resistance and ultimate deformability of structures acted on by well defined repeated loads, Lisbon, 1973, pp. 15-22.
[14] S.K. Kunnath, A. El-Bahy, A.W. Taylor, W.C. Stone, Cumulative Seismic Damage of Reinforced Concrete Bridge Piers, NIST Interagency/Internal Report (NISTIR) 1997.
[15] E. ASTM, 1049-85, Standard practices for cycle counting in fatigue analysis, ASTM Standards, 2005, pp. 614-620.
[16] R.P. Dhakal, K. Maekawa, Reinforcement stability and fracture of cover concrete in reinforced concrete members, Journal of Structural Engineering-ASCE 128(10) (2002) 1253-1262.
[17] M.A. Miner, Cumulative damage in fatigue, Journal of Applied Mechanics 12 (1945) A159-A164.
[18] S. SeismoSoft, A computer program for signal processing of strong-motion data, 2010.
[19] NZS1170.5, Structural design actions: Part 5, Earthquake actions, 2004.